

Propagation of solitons of the magnetization in magnetic nano-particle arrays

Satoshi Ishizaka and Kazuo Nakamura
*NEC Fundamental Research Laboratories,
 34 Miyukigaoka, Tsukuba, Ibaraki, 305, Japan*
 (February 1, 2008)

It is clarified for the first time that solitons originating from the dipolar interaction in ferromagnetic nano-particle arrays are stably created. The characteristics can be well controlled by the strength of the dipolar interaction between particles and the shape anisotropy of the particle. The soliton can propagate from a particle to a neighbor particle at a clock frequency even faster than 100 GHz using materials with a large magnetization. Such arrays of nano-particles might be feasible in an application as a signal transmission line.

The recently developed nanofabrication techniques make it possible to fabricate ferromagnetic particles to a length of 20-30 nanometers.¹ Since the size of such nano-particles is small enough to be a single domain, the magnetization is homogeneous over a particle and can be described by a magnetic moment. These particles interact with each other due to a dipolar interaction of the magnetic moments. In such a nano-particle, the magnetic anisotropy energy can be dominated by the particle's shape rather than the magnetocrystalline anisotropy. Therefore, the magnetic anisotropy energy can be well controlled by changing the shape of the particle. When the distance between particles is short enough that dipolar interaction becomes comparable with the anisotropy energy, the direction of the magnetization of each particle is determined in order to minimize both energies, and the direction of the magnetization moves in a corrective manner among the particles.

It is known that the magnetic domain wall in bulk magnetic materials is a kind of solitons of nonlinear waves.²⁻⁴ Usually, the soliton originates from the exchange interaction between spins. This letter clarified for the first time that, in a one-dimensional array of nano-particles, solitons originating from the dipolar interaction between particles are present, and that the characteristics can be well controlled by the strength of the dipolar interaction and the shape anisotropy. The great advantage of control is quite a contrast to the case of the soliton of the domain walls in bulk materials.

In this letter, we analyze the characteristics of the solitons in arrays of ferromagnetic nano-particles by varying the experimentally controllable parameter: the shape anisotropy energy. When the damping is small, the soliton propagates from a particle to a neighbor particle at 50 GHz, even faster than 100 GHz using materials with a large magnetization. Such arrays of nano-particles might

be feasible in an application as a signal transmission line.

We examine a one-dimensional array of particles in the x -direction. Each particle has a magnetic moment \vec{M}_i ($|\vec{M}_i| = M$). The dipolar interaction and anisotropy energy is modeled as

$$H = \sum_{\langle ij \rangle} \frac{\mu_0}{4\pi r_{ij}^3} [\vec{M}_i \cdot \vec{M}_j - \frac{3}{r_{ij}^2} (\vec{M}_i \cdot \vec{r}_{ij})(\vec{M}_j \cdot \vec{r}_{ij})] + \sum_i \frac{1}{M} [-K_y M_{iy}^2 + K_z M_{iz}^2], \quad (1)$$

where K_y and K_z describe the shape anisotropy. The dipolar interaction is characterized by $J = \mu_0 M^2 / (4\pi a^3)$. In this letter, we consider the case of $K_z \gg J$ and $K_z \gg K_y$, and thus the $x-y$ plane is an easy plane for the magnetization. Further, we consider the case where the thermal fluctuation in the direction of \vec{M}_i , which frequently leads to the super-paramagnetism,⁶ is well-suppressed by K_y and/or J . As shown below, the condition can be sufficiently satisfied since J can exceed 10,000 K even for particles of a size of 20 nm, when these are aligned closely to each other.

The magnetization of each nano-particle obeys the Bloch equation:⁷

$$\frac{d\vec{M}_i}{dt} = -\frac{\nu}{M} \vec{M}_i \times \left(-\frac{\partial H}{\partial \vec{M}_i} - \frac{\alpha M}{\nu} \frac{d\vec{M}_i}{dt} \right), \quad (2)$$

where $\nu = g\mu_B/\hbar$ is a gyromagnetic constant, and α describes the dumping due to energy dissipation, such as magnetoelastic dissipation and eddy current loss in metallic ferromagnets. In nano-particles, however, it has been shown that the amount of these dissipation mechanisms are negligibly small.^{8,9} In fact, considering the eddy current loss, $\alpha \sim 10^{-4}$ for Fe-particles of a size of 20 nm, for which the soliton can propagate beyond 1,000 sites. Therefore, we exclusively consider the case of $\alpha = 0$ in this letter.

Before discussing the results of the numerical simulations of Eq. (2), it is worth considering the continuum limit. There are two types of configurations of \vec{M}_i giving the minimum total energy depending on K_y . When only the nearest-neighbor interaction is considered for simplicity, the configuration is type I [Fig. 1 (a)] and type II [Fig. 1 (b)] for $K_y < J$ and $K_y > J$, respectively. In both cases, the Bloch equation (2) is approximated to the sine-Gordon (SG) equation:⁵

$$\nabla^2 \theta'(x, t) - \frac{1}{c^2} \frac{\partial^2 \theta'(x, t)}{\partial t^2} - \frac{1}{\lambda^2} \sin \theta'(x, t) = 0, \quad (3)$$

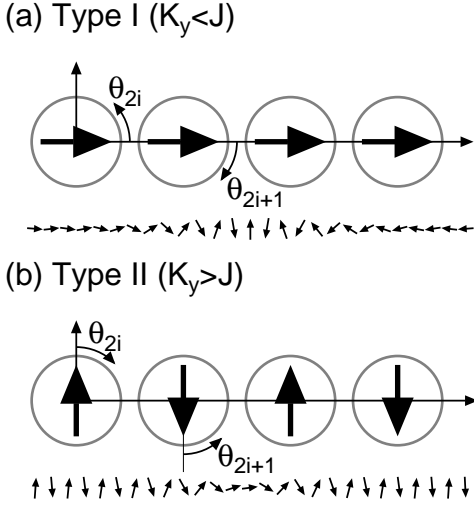


FIG. 1. The configuration of the magnetization giving a minimum total energy. (a) type I for $K_y < J$ and (b) type II for $K_y > J$. For both cases, an example of the soliton is shown below each figure.

where $c^2 = 3Ja^2K_z\nu^2/M^2$, $\lambda^2 = 3Ja^2/(4|K_y - J|)$, and $\theta'(x, t)/2 = \theta(x, t)$ is the azimuthal angle of $\vec{M}(x)$ in the continuum limit of \vec{M}_i . Note that the definitions of θ_i for even- and odd-sites are different as shown in Fig. 1. Consequently, the solution in the form of the soliton is present for both cases of type I and II, whose examples are shown below Figs. 1 (a) and (b). The solution has a velocity (v) as a parameter, and its wavelength is $l = \lambda\sqrt{1 - v^2/c^2}$. The maximum velocity is limited to c .

When the long range part of the interaction is taken into account, $|K_y - J|$ in λ^2 is replaced by $|K_y - 5\zeta(3)J/4| \approx |K_y - 1.5J|$ with $\zeta(x)$ being Riemann's zeta function. To gain a large value of J , however, it is better to align particles closely in such a way that the distance between particles (a) is comparable with the diameter of the dot (d), where the nearest-neighbor interaction becomes dominant. Therefore, we only take into account the nearest-neighbor interaction in Eq. (1) hereafter, although the actual form of the interaction may slightly deviate from that in Eq. (1) for $a \sim d$.

Figure 2 shows the time-evolution of the center coordinate of the soliton obtained from the numerical calculations of Eq. (2) for various values of K_y . As an initial condition for $t = 0$, we choose a solution of SG-equation (3) with an initial velocity $v = 0.2c$. For both cases of type I and II, the soliton stably propagates keeping the initial velocity when K_y is close to J . The velocity begins to decrease when $|K_y - J|$ becomes large, and the amount of the decrease is more significant for the case of type II than type I. The soliton for type II stops after the propagation beyond 30 sites for $K_y = 1.2J$, while the soliton for type I can propagate even for $K_y = 0$. Therefore, the configuration of type I with K_y close to J is suitable for the stable propagation of the soliton.

We performed the same calculations for the type I case

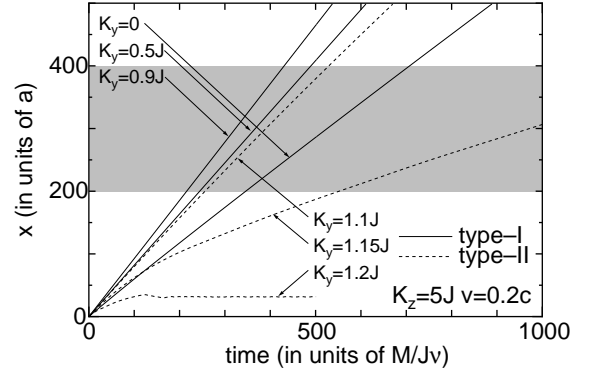


FIG. 2. The time-evolution of the center coordinate of the soliton for various values of K_y . Solid and dotted lines are for type I and type II, respectively. A gray zone shows the range ($200 \leq x \leq 400$) where the average velocity plotted in Fig. 3 (a) is obtained.

for various values of the initial velocity, and obtained the average velocity (\bar{v}) in the range, for example, of $200 \leq x \leq 400$. The results are shown in Fig. 3 (a). The average velocity \bar{v} keeps the initial velocity for smaller velocities. This implies that the solution of the continuum limit is appropriate for this range of the velocity. With the increase of the initial velocity, however, the effects of the discreteness of the array become important, and \bar{v} begins to saturate and comes to depend little on the initial velocity. With the further increase of the initial velocity, \bar{v} for $K_y \geq 0.3J$ increases suddenly with a finite jump, and \bar{v} takes an almost completely fixed maximum value. It is interesting to note that the corresponding wavelength of the soliton is always close to the distance between particles (a) independent of K_y , while the corresponding fixed value of \bar{v} depends on K_y . In the case of $K_y \leq 0.1J$, although the jump becomes very broad and the velocity is not fixed so rigorously, similar behavior also remains. It should be noted that the sudden jump and fixing in the velocity is absent in the case of type II.

According to the numerical results, the maximum of the average velocity (v_c) and the corresponding wavelength (l_c) satisfies an approximate relation similar to the continuum limit:

$$\left(\frac{v_c}{c}\right)^2 + \left(\frac{l_c - 0.25a}{\lambda}\right)^2 = 0.76, \quad (4)$$

as shown in the inset of Fig. 3. Therefore, due to the effects of the discreteness of the array, the wavelength is shifted by a constant, and c and λ are renormalized simultaneously, although the amount of the shift and the renormalization may depend on the distance of the soliton propagation. The corresponding wavelength l_c is always close to a as discussed above. Therefore, the maximum velocity of the soliton is approximately given by K_y as

$$v_c \approx c\sqrt{0.01 + 0.75\frac{K_y}{J}}. \quad (5)$$

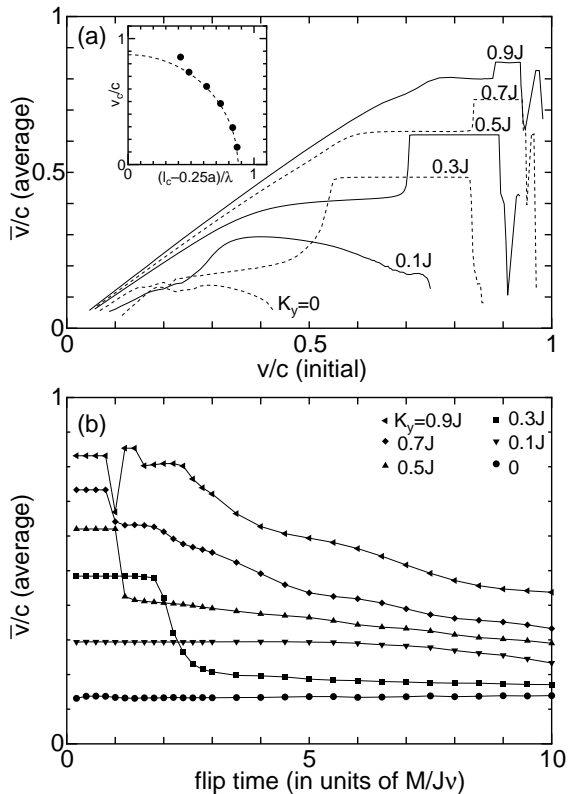


FIG. 3. (a) The average velocity obtained for the range $200 \leq x \leq 400$ as a function of initial velocities. The inset shows the relation between the maximum of the average velocity (v_c) and the corresponding wavelength (l_c). (b) The average velocity of the soliton generated by flipping \vec{M}_0 as a function of the flipping time. The average is performed in the range of $200 \leq x \leq 400$.

It is possible to generate similar solitons when the magnetization at the edge of the array (\vec{M}_0) is simply rotated and flipped by an external force. In fact, the average velocity of the solitons generated in such a way is plotted in Fig. 3 (b) as a function of the flipping time. When flipping is faster than $M/J\nu$, the average velocity is fixed without regard to the flipping time. The corresponding wavelength of the soliton is also fixed to a , and the velocity is approximately given by Eq. (5) again. For slower flipping time ($> 3M/J\nu$), the average velocity gradually decreases with the increase of the flipping time, and we have checked that the soliton can be generated even for much slower flipping time ($\sim 100M/J\nu$).

Finally, we mention the actual values of parameters for an experimental setup. It is better to align particles closely ($a \sim d$) in order to gain a large J as discussed before. Since the particle is a single domain, $M \propto d^3$, and thus $J \propto M^2/a^3 \propto d^3$. Therefore, J decreases with the decrease of the size of the particle. For a cylinder of Fe with $d = 20$ nm and a height of 10 nm, however, J is as large as $J \sim 2 \times 10^4$ K. The soliton propagates to the nearest-neighbor site in a time of $t_0/\sqrt{3K_z/J}$ with $t_0 \equiv M/(J\nu)$, which does not depend too much on d . For

an Fe-particle of the above size, $t_0/\sqrt{3K_z/J} \sim 2 \times 10^{-11}$ sec (~ 50 GHz) assuming $K_z/J = 5$. The maximum velocity in the continuum limit is $c = \sqrt{3K_z/J}(a/t_0) \sim 1 \times 10^3$ m/s for $a = 20$ nm. When the particles are fabricated to have a shape anisotropy of $K_y \sim 0.7J$, the actual velocity is about 70% of c according to Eq. (5). Since the clock frequency shown above is proportional to the magnetization, it might be able to exceed 100 GHz for materials with a large magnetization.

To conclude, we have shown for the first time that a soliton excitation mode is present in magnetic nanoparticle arrays with the dipolar interactions for both configurations of the magnetization (type I and type II) giving the minimum total energy depending on the shape anisotropy. The soliton mode in the type I configuration exists in a wider range of the shape anisotropy than that in the type II configuration. The solitons with the maximum velocity, which depend on the shape anisotropy, always have a wavelength close to the distance between particles. These solitons are stable independent of the initial conditions, and they can be generated by fast flipping of the magnetization at the edge of the array. The soliton can propagate from a particle to a neighbor particle at a clock frequency even faster than 100 GHz, and may be feasible in an application as a signal transmission line.

Finally, it should be noted that the dominant mechanism of the dumping in the nano-particle arrays and the effects of the disorder in the alignment of the particles and its shape are not clarified yet. Further intensive studies will be necessary on these effects.

We would like to thank Takeshi Honda, Jun-ichi Fujita, and Toshio Baba for helpful discussions.

¹ Y. Honda and J. Fujita, unpublished.

² U. Enz, *Helv. Phys. Acta* **37**, 245 (1964).

³ H. Mikeska and E. Patzak, *Z. Phys.* **B26**, 253 (1977);

H. Mikeska, *J. Phys. C* **11**, L29 (1978).

⁴ *Solitons and Condensed Matter Physics*, edited by A. R. Bishop and T. Schneider (Springer-Verlag, New York, 1981).

⁵ see for example, P. K. Dodd, J. C. Eilbeck, J. D. Gibbon, and H. C. Morris, *Solitons and Nonlinear Wave Equations* (Academic press, London, 1982).

⁶ C. P. Bean and I. S. Jacobs, *J. Appl. Phys.* **27**, 1448 (1956).

⁷ T. L. Gilbert, *Phys. Rev.* **100**, 1243 (1955).

⁸ G. Tatara and H. Fukuyama, *Phys. Rev. Lett.* **72**, 772 (1994).

⁹ A. Grag and G-H. Kim, *Phys. Rev. Lett.* **63**, 2512 (1989); A. Grag and G-H. Kim, *Phys. Rev.* **B43**, 712 (1991).